# Modeling the Effects of Deformable Mirror Location in the OMEGA EP Pulse Compression System

John Jamieson

**Allendale Columbia School**
Pittsford, NY

Advisor: Mark Guardalben

**Laboratory for Laser Energetics**
University of Rochester
Rochester, NY

# Modeling the Effects of Deformable Mirror Location in the OMEGA EP Pulse Compression System

**Abstract:**

The wavefront of the OMEGA EP laser beam within the pulse compression system is corrected using a deformable mirror (DM) located after the last grating of the pulse compressor. A spatio-temporal numerical model (EPCOMP) was used to investigate whether the DM could be moved to a location before the first grating of the compressor. This would reduce the peak power incident on the DM by a factor of 1000. In the model, measured surface deformations were applied to the seven mirrors that transport the beam from the output of the compressor to the target chamber and a DM correction was applied to produce a focal spot size of 2.4 microns at 80% encircled energy (R80) and a pulse width close to its transform-limited value of 0.52 ps for both DM locations. A two-grating analytical model was used to confirm that the spectral phase distortion at the output of the compressor was indeed negligible for the expected wavefront error introduced by DM pre-correction.

## 1. Introduction

The two short-pulse beamlines of the OMEGA EP laser system use chirped-pulse amplification (CPA) [1] to achieve on-target intensities that exceed $10^{24}$ Watts per square meter in a picosecond pulse. The CPA technique, shown in Figure 1, is used to reduce the risk of laser damage to optics in the beamlines by first stretching a pulse in time, amplifying it through flashlamp-pumped Nd-doped glass disks, and then compressing it using a four-grating pulse compressor before propagating it to the target. Each of the four diffraction gratings used in the OMEGA EP pulse compressor comprises three smaller, tiled gratings because of the cost and technical challenges involved in implementing larger, meter-size gratings [2].

After pulse compression, the laser beam is transported through a series of mirrors to the target chamber. Because the compressor gratings and transport mirrors are not perfectly flat, each will introduce a wavefront error onto the beam that will degrade its focal spot quality if left uncorrected. The deformable mirror (DM), currently located after the last grating of the compressor, is used to correct the wavefront errors. The DM has 39 pistons behind it that can push and pull the glass of the DM and physically "mold" it to be the optimal shape for wavefront correction. The purpose of this project was to determine whether or not the DM could be moved to before the compressor without introducing excessive spectral phase errors that could degrade the compressed pulse, leading to reduced on-target intensities. Doing so would reduce the power on the mirror by a factor of 1000, substantially reducing the risk of further laser-induced damage on the DM.

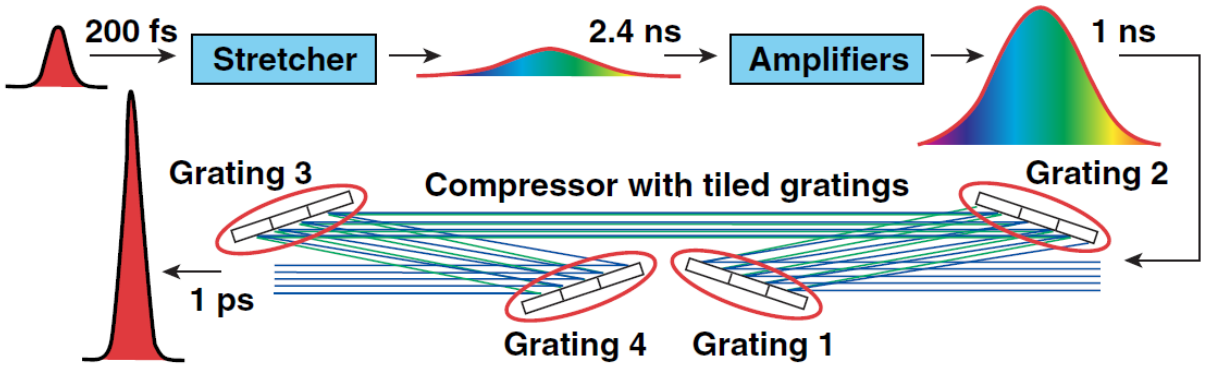


Figure 1 – **Chirped Pulse Amplification (CPA)** – Block diagram of the CPA technique used in OMEGA EP. The laser pulse is first stretched in time, amplified, and then compressed using a four-grating pulse compressor. The pulse stretcher stretches the pulse by delaying each color of the pulse spectrum by a different amount. The compressor produces a short pulse by bringing these colors back together in time.

## 2. EPCOMP Numerical Model

EPCOMP is a three-dimensional beam propagation code that is used to model the OMEGA EP tiled-grating pulse compressor. It uses the commercial software package FRED [3] as a non-sequential ray-tracing engine and performs coherent propagation using the Gaussian beamlet method [4]. The OMEGA EP pulse spectrum was assigned to each spatial point in the EPCOMP source grid and each spectral slice of the beam was propagated through the compressor and transport sections of OMEGA EP. The electric field of each spectral slice was coherently sampled on a rectilinear grid that was placed in two different locations. The near-field beam was sampled between the last transport mirror and the off-axis parabola (OAP) focusing element, and the far-field beam was sampled at the center of the OMEGA EP target chamber. A MATLAB [5] post-processor was used to calculate the temporal pulse from the pulse spectrum at each grid point, and can provide detailed predictions of the temporally resolved near-field and far-field beams.

The wavefront error incurred through the transport section was sampled at the central wavelength of the pulse spectrum just prior to the OAP. The DM surface height distribution necessary to correct this wavefront error was determined using an experimentally calibrated DM influence function model [6] and then applied to the deformable mirror surface in the FRED model as a bicubic mesh.

Figure 2 shows the FRED model that was used. The figure four at the input to the compressor does not currently exist in the actual laser system, but is a proposed configuration for the DM that would be located there.

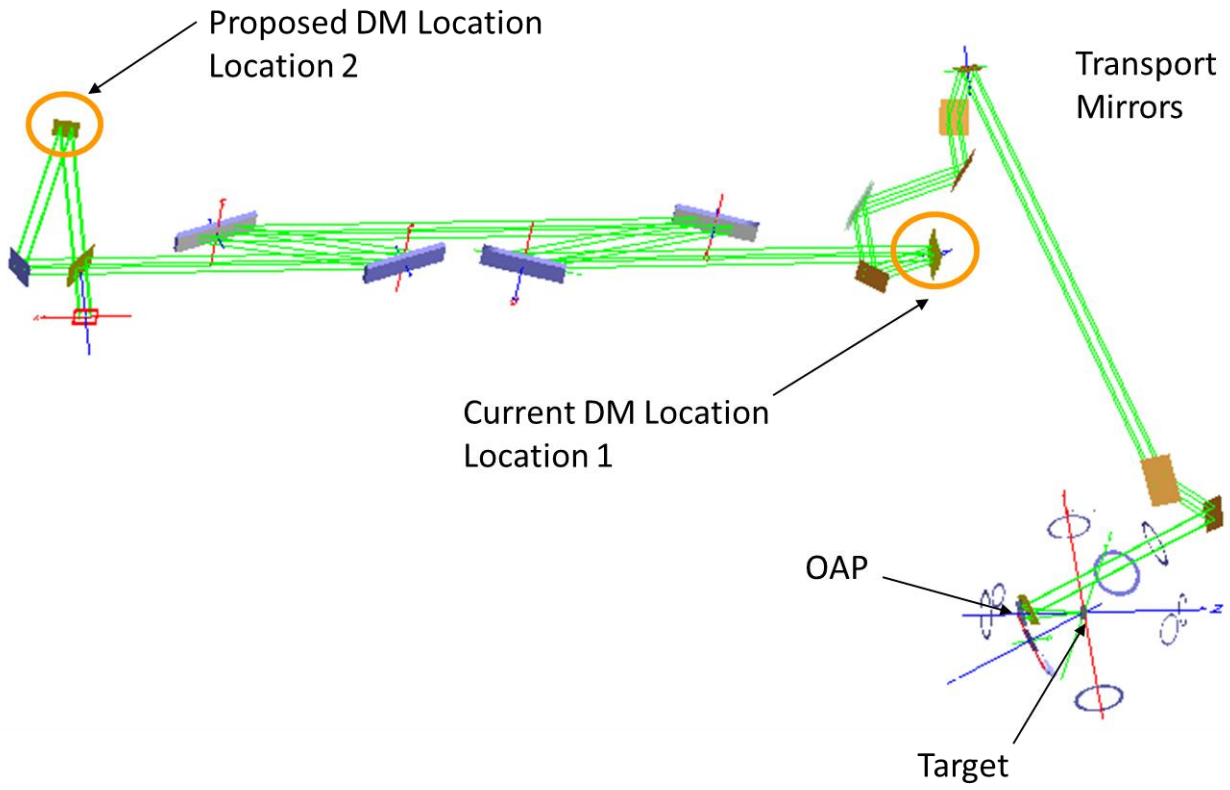


Figure 2 – **The FRED Model** - The beam was propagated through two mirrors arranged in a figure four, the four-grating compressor, and the transport section, and was focused onto the target using the off-axis parabola mirror (OAP). Location 1 is where the DM currently is located. Location 2 at the input to the compressor is the proposed DM location. The first mirror after the source was 100% reflecting when the DM was in Location 1, but 100% transmitting when the DM was in Location 2.

The temporally integrated focal spot was characterized using the 80% encircled energy radius (R80), which is the minimum radius of a circle that contains 80% of the energy in the focused beam. A smaller R80 is more desirable because it means that higher on-target intensities can be achieved. The spatially integrated pulse was characterized by its full width at half of its maximum value (FWHM). The transform-limited FWHM was 521 fs using a Gaussian spectrum with spectral width close to that of the amplified, on-shot OMEGA EP spectrum.

The spectral phase of the pulse represents how spread out the pulse spectrum is (see Figure 1). The spectral phase of the pulse entering the compressor for a perfectly matched stretcher and compressor was obtained by propagating the spectral pulse that had a uniform spectral phase profile through the compressor and transport system with no alignment or wavefront errors. The conjugate of the accumulated spectral phase of the output pulse was then assigned to the input pulse for subsequent modeling runs. The beam was modeled using a 36.9-cm square aperture source grid of 30x30 uniformly weighted rays.

## 3. Results

### 3.1 The Perfect System

The perfect system with no wavefront error or DM correction was modeled first to provide a baseline against which to compare subsequent modeling runs. These results are shown in Figure 3. With no wavefront error on the beam, the focal spot R80 was 2.4 microns, and the compressed pulse FWHM was 0.52 ps.

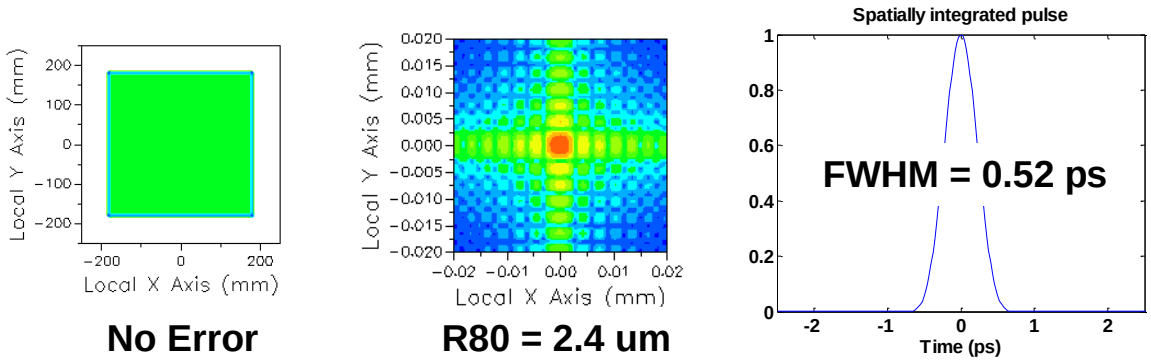


Figure 3 – **The Perfect System** The left plot displays the wavefront after the last mirror. The central plot is a log plot of the irradiance at the target, with 6 orders of magnitude represented by the color map used. Red regions in the central plot are areas of highest light intensity and blue regions are areas of lowest light intensity. The right plot is the spatially integrated pulse at the target. There is no error on the wavefront, the R80=2.4 microns, and the FWHM of the pulse is 0.52 ps.

### 3.2 Transport Mirror Error with No DM Correction

Measured surface errors were applied to the transport mirrors in the FRED model as third-order x, y polynomials with no DM correction for this run. Figure 4 shows that the peak-to-valley wavefront and R80 increased to 0.63 waves and 3.7 microns, respectively, but there was no difference in the FWHM pulse width compared to the perfect system.

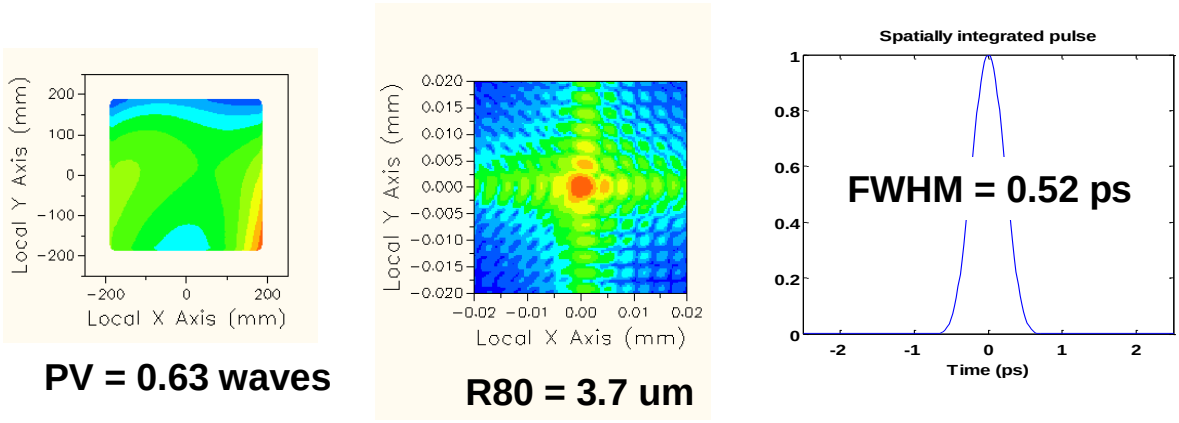


Figure 4 – **Transport Error with No DM Correction** –Measured surface deformations from the transport mirrors were applied to the perfect system. The left plot displays the wavefront after the last mirror. The central plot is a log plot of the irradiance at the target. The right plot is the spatially integrated pulse at the target. There is a peak-to-valley error of 0.63 waves on the wavefront, the R80 is increased to 3.7 microns, and the FWHM=0.52 ps.

### 3.3 DM Correction at Compressor Output

In this run, the influence function model was used to generate a DM correction for the wavefront error of section 3.2 that was applied to the DM at the output of the compressor. The DM was able to correct the focal spot R80 from 3.7 microns back down to the level of the perfect case, 2.4 microns, as shown in Figure 5. The left plot in Fig. 5 shows that the residual wavefront error had a peak-to-valley of 0.08 waves, with a spatial pattern arising from the finite distance between DM pistons, each piston being modeled by the influence function. The pulse width was not affected by the DM after the compressor.

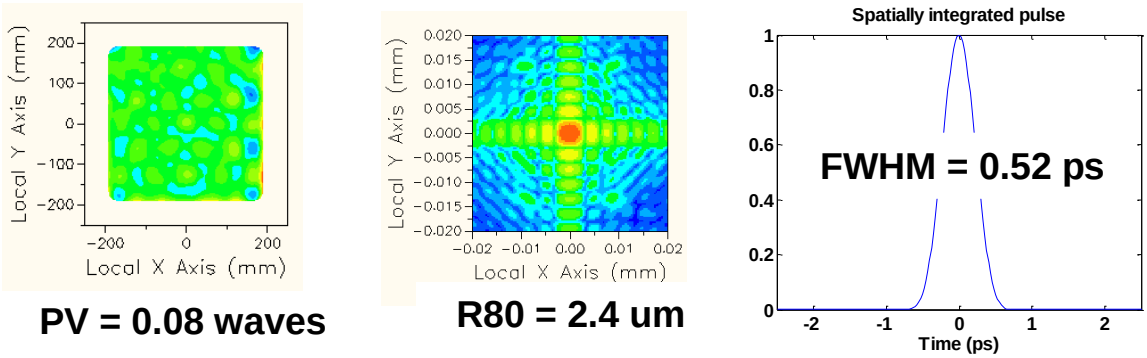


Figure 5 – **DM Correction After Compressor** – The DM correction was applied after the compressor. The left plot shows that there is a peak-to-valley residual wavefront error of 0.08 waves. The central and right plots respectively show that the R80=2.4 microns, and the compressed pulse FWHM=0.52 ps.

### 3.4 DM Correction at Compressor Input

In this run, the influence function model was used to generate a DM correction for the wavefront error of section 3.2 that was applied to the DM at the input of the compressor. The R80, peak-to-valley residual wavefront error, and compressed pulse FWHM were the same as for DM correction at the output of the compressor. These results are summarized in Figure 6.

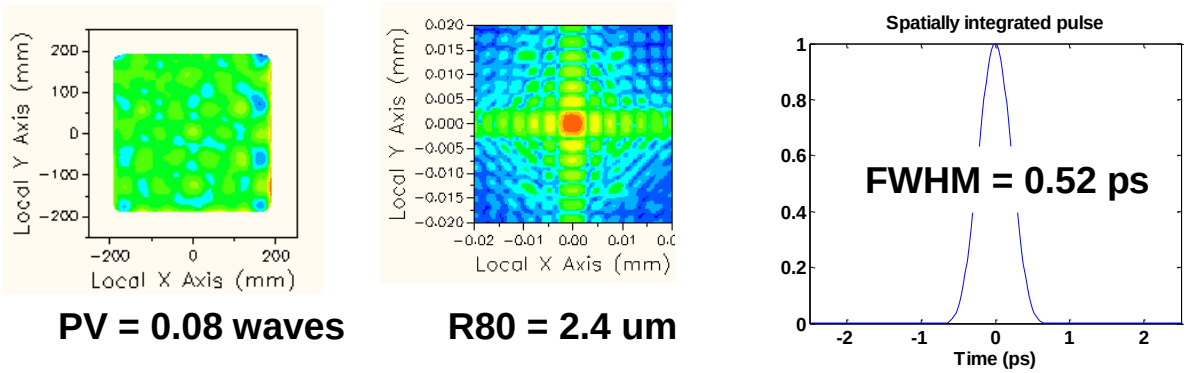


Figure 6 – **DM Correction Before Compressor** – The DM correction was applied before the compressor. There is a peak-to-valley residual wavefront error of 0.08 waves, the R80=2.4 microns, and the FWHM=0.52 ps.

## 4. Model of DM-Corrected Rays

One concern with placement of the DM before the grating compressor was that the compressed pulse might be distorted due to the different paths of the DM-corrected rays through the compressor. This is illustrated in Figure 7, where the dashed path represents a DM-corrected ray through a grating pair. The deviation of the DM-corrected ray (of order 10 microradians for the largest seen in Section 3) is greatly exaggerated in the figure. This effect was calculated for a two-grating system by working out the exact ray paths as shown in Figure 7, for each frequency in the pulse spectrum, and integrating over the spectrum using the method described in reference [7].

The delay for wavefront gradient errors (i.e., ray direction errors) is shown in the right plot of Figure 8. The delay is less than 8 as (1 as = $10^{-18}$ s). The left plot of Figure 8 shows that the temporal pulses calculated with and without the wavefront gradient errors are virtually identical.

The results of Figure 8 confirm that a DM that pre-corrects errors in front of the pulse compressor will lead to negligible pulse broadening in the OMEGA EP laser system.

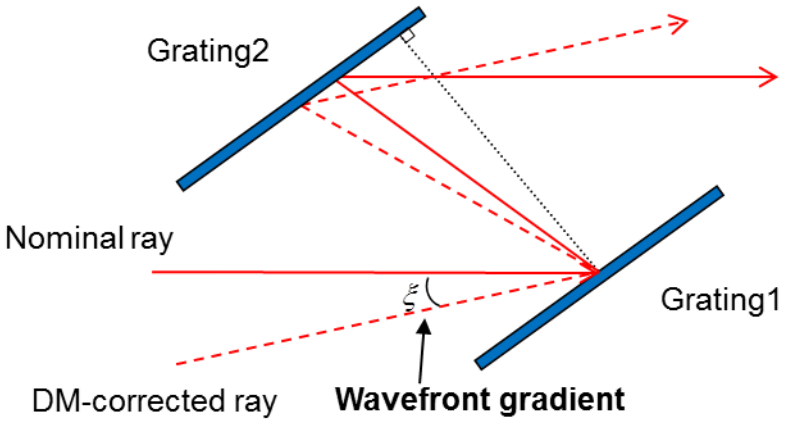


Figure 7 – **Two-Grating Model** – The paths of a nominal ray and a DM-corrected ray with the same frequency are shown.

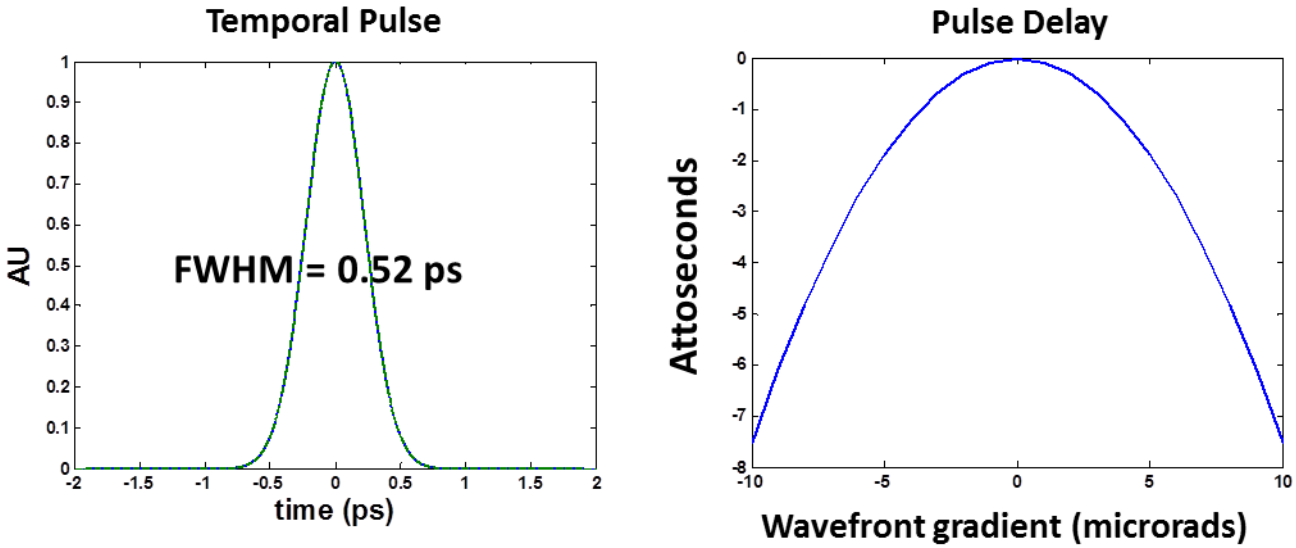


Figure 8 – **Temporal Pulse and the Pulse Delay**–The graph on the left is a spatially integrated pulse, showing virtually identical results with and without a 10 microradian change in wavefront direction due to DM corrections (solid and dotted lines are with and without DM correction, respectively). The plot on the right shows the relationship between the deviation in incoming wavefront direction (in microradians) and the pulse delay in as. This displays that a 10 microradian error would give less than 8 as delay.

## 5. Conclusion/Further Work

The spatio-temporal numerical model showed that a DM can correct for expected errors in the wavefront just as well when placed before the compressor as after the compressor. Both deformable mirrors corrected the wavefront errors sufficiently to recover the perfect-system focal spot R80 of 2.4 microns, while keeping the compressed pulse FWHM at its transform-limited value of 0.52 ps. A two-grating analytical model was used to confirm that the spectral phase distortion was indeed negligible.

To improve the simulation, the model will be expanded to include errors from the main beamline and the diffraction gratings. The effect of DM pre-correction on pulse contrast will also be explored. Finally, engineering considerations for moving the DM, such as opto-mechanical constraints of the system, implications for compressor alignment, and cost will also be investigated.

## 6. Acknowledgements

I would like to thank Dr. R. Stephen Craxton and the Laboratory for Laser Energetics for providing me with the opportunity to spend a summer doing research. I would like to thank my advisor M. Guardalben for advice, knowledge, and guidance throughout the procces. I would also like to thank B. Kruschwitz for creating the DM model used to create the bicubic meshes.

## 7. References

1. D. Strickland and G. Mourou, “Compression of amplified chirped optical pulses,” Opt. Commun. **56**(3), 219–221 (1985).

2. J. Qiao, A. Kalb, M. J. Guardalben, G. King, D. Canning, and J. H. Kelly, "Large-aperture grating tiling by interferometry for petawatt chirped-pulse–amplification systems," Opt. Express **15**, 9562-9574 (2007) http://www.opticsinfobase.org/oe/abstract.cfm?URI=oe-15-15-9562
3. Photon Engineering, LLC, Tucson, AZ 85751.
4. J. Arnaud, "Representation of Gaussian beams by complex rays," Applied Optics, **24**(4), 538-543 (1985).
5. MathWorks, Natick, MA 01760.
6. MATLAB DM influence function model provided courtesy of Brian Kruschwitz.
7. Z. Wang, Zh. Xu, and Zh. Zhang, "A new theory for the treatment of a pulsed beam propagating through a grating pair," IEEE J. Quantum. Electron. QE-**37**(1), 1-11(2001).